With this expression for $I_2(l)$, the third factor becomes $\exp[I_2(l)]$. Finally, terminating the series exponential in Eq. (24) with the second term, we get

$$T(l)=\exp[-\gamma L^2+I_1(l)+I_2(l)]. \tag{A50}$$

If we omit the $I_2(l)$ term from this expression the result

$$T(l)\cong\exp\{-\gamma L^2+I_1(l)\} \tag{A51}$$

is referred to as the first approximation to $T(l)$. Then in this sense, the second approximation to $T(l)$ is given by Eq. (A50).

PHYSICAL REVIEW VOLUME 149, NUMBER 1 9 SEPTEMBER 1966

Investigation of Electronic Recombination in Helium and Argon Afterglow Plasmas by Means of Laser Interferometric Measurements*

M. A. GUSINOW,† J. B. GERARDO,‡ AND J. T. VERDEYEN
Gaseous Electronics Laboratory, Department of Electrical Engineering, University of Illinois, Urbana, Illinois

(Received 4 April 1966; revised manuscript received 11 May 1966)

Two helium-neon laser interferometers were used to obtain the electron and neutral-atom densities in an afterglow plasma. The interferometric technique utilized allows one to obtain both the spatial and temporal dependence of the electron decay. The two gases studied were helium and argon at 2–8 Torr and 0.3–0.8 Torr, respectively. The electron density was in the range of $2\times10^{13}<N_e<10^{15}$ cm^{-3} and the electron temperature in the range $1000<T_e<7000$°K. The electron temperature was measured by comparing the relative atomic line intensities and by inference from the recombination coefficient. The electronic recombination in helium, argon, and helium-argon mixtures was found to be consistent with the predictions of Bates, Kingston, and McWhirter for collisional-radiative recombination. The electron temperature inferred from the measured recombination coefficient indicates a pronounced electron temperature gradient across the tube which is believed to be due to electron heating effects in the afterglow.

INTRODUCTION

ELECTRONIC recombination in gaseous plasmas has been the subject of numerous studies dating back to the early part of the twentieth century. In spite of the tremendous amount of attention focused on this phenomenon, there are still many questions that remain to be answered. One of the major advancements made in the understanding of electronic recombination was the proposal by Bates[1] that dissociative recombination may play a leading role in the recombination process. Whereas the importance of this phenomenon is well documented, it has become increasingly apparent that other processes may be of significance. One of these is the three-body collision of two free electrons and a positive ion resulting in an excited neutral atom. Also of great importance is the effect of electron collision which excited atoms. It has been shown that inclusion of such collisions enhances recombination.[2,3] The net effect has been coined collisional radiative recombination.

Collisional-radiative recombination was put on a firm theoretical foundation by Bates *et al.*[3] It was subsequently shown, within a limited range of plasma parameters, that their results described the recombination process in helium,[2] hydrogen,[4] and cesium.[5]

In this work we extended the range of plasma parameters over which collisional-radiative recombination is expected to be the dominant recombination process in helium plasmas. The results of Bates are also shown to apply to argon and helium-argon plasmas.

In the work described here, the plasmas were formed in helium and argon gases in the pressure ranges 3–8 Torr and 0.2–0.8 Torr, respectively, by an electrode type of capacitor discharge. This resulted in a plasma with an electron density $N_e\approx10^{15}$ cm^{-3} and $T_e\approx7000$°K immediately after cessation of the active discharge. Both N_e and T_e subsequently decay during this afterglow.

* Work supported by the U. S. Army Research Office, Durham, North Carolina.
† Submitted in partial fulfillment for the degree of Doctor of Philosophy.
‡ Present address: Sandia Corporation, Albuquerque, New Mexico.
[1] D. R. Bates, Phys. Rev. **77**, 718 (1950).
[2] E. Hinnov and J. G. Hirschberg, Phys. Rev. **125**, 795 (1962).
[3] D. R. Bates, A. E. Kingston, and R. W. P. McWhirter, Proc. Phys. Soc. (London) **83**. 43 (1964).
[4] W. S. Cooper and W. B. Kunkel, Phys. Rev. **138**, 1022 (1965).
[5] Yu. M. Aleskovskii, Zh. Eksperim. i Teor. Fiz. **44**, 840 (1963) [English transl.: Soviet Phys.—JETP **17**, 570 (1963)].

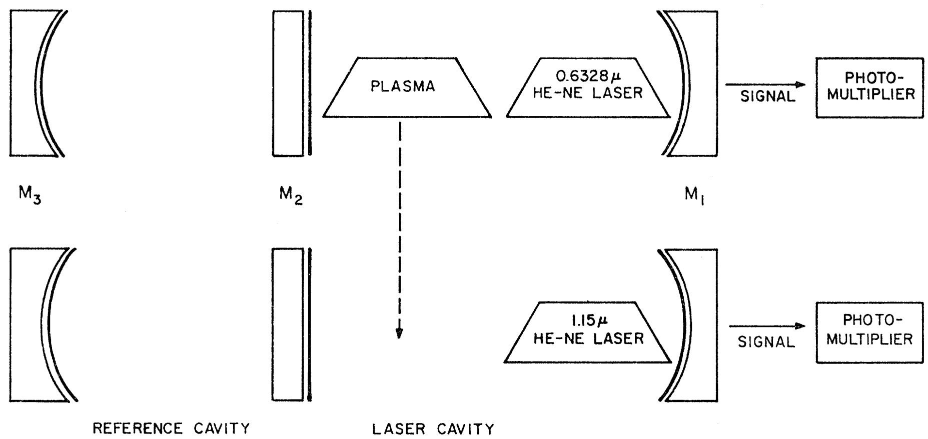

FIG. 1. Experimental arrangement of laser interferometers.

It was found that there was a nonuniform electron-temperature distribution across the discharge tube in the afterglow. This was inferred from the experimentally determined spatially resolved recombination coefficient. This nonuniformity is attributed to nonuniform heating of the electron gas by recombination and metastable heating in the afterglow. Whereas such heating effects have previously been considered by many investigators, to the best of our knowledge this is the first time that spatially inhomogeneous heating has been considered. We discuss the effect of this nonuniform heating on diffusion and recombination.

EXPERIMENTAL TECHNIQUE

The primary diagnostic tool used in this investigation was the laser interferometer. This device allows one to obtain spatially resolved plasma-electron densities. Since the theory of the interferometer has been adequately described elsewhere, only those features which make it particulary suitable for these studies here will be reviewed.[6,7]

The interferometer arrangement is illustrated in Fig. 1. With the plasma located in the laser cavity, cross-sectional spatial resolution of less than 1 mm^2 can be obtained. If we assume that the polarizability of the neutral atom, including excited states, is independent of wavelength, then two-wavelength interferometry is sufficient to determine the plasma electron density. If one also assumes that the degree of ionization is small and that the number of excited states is small in comparison to the number of ground-state atoms, or that the polarizatiblity of these excited states is essentially equal to that of the ground state atoms, then these measurements are also sufficient to measure the neutral-atom density. The validity of these assumptions for the type of plasma investigated here, for $2\times10^{13}\leq N_e \leq 8\times10^{13}$, has previously been shown by simultaneous measurement of the electron density utilizing a microwave-transmission technique.[8]

The electron temperature in the afterglow was measured by comparison of relative spectral-line intensities. The helium transitions used were: 10^1D-2^1P, 8^1D-2^1P, and 5^1D-2^1P. Under the experimental conditions the upper states of the first two transitions were expected to be in local thermodynamic equilibrium (LTE)[9,10] with the free-electron gas. The 5^1D state was expected to be in only approximate LTE with the continuum electrons. The argon transitions employed were: $3p_1$-$1s_2$, $3p_5$-$1s_2$, and $3p_2$-$1s_3$. None of these upper states were expected to be in LTE with the continuum. However, the spacing between these upper states is not greater than 0.162 eV and similar to Robben *et al.*[11] it was expected that due to electron collisions the relative populations of these upper states would be described by the Boltzmann factor $\exp(-E_i/kT)$ where E_i is the energy of the ith state relative to the lowest level under consideration. The temperature describing this distribution is that of the free-electron gas. The spectral temperatures obtained were also spot-checked by Langmuir-probe techniques and good agreement was found. The accuracy of such spectral determinations of electron temperature is discussed in Ref. 12.

The plasma vessel used in this work was 47 cm long with an inside diameter of 1.2 cm. The plasma was produced by discharging a capacitor through a gas filling the tube. A tungsten hot cathode was used. Provision was made to clamp (crowbar) the discharge current at any

[6] J. B. Gerardo, J. T. Verdeyen, and M. A. Gusinow, University of Illinois Science Report No. 1, Grant No. DA-ARO-D-31-124-G582, 1964 (unpublished).

[7] J. B. Gerardo, J. T. Verdeyen, and M. A. Gusinow, J. Appl. Phys. **36**, 3526 (1965).

[8] J. B. Gerardo and J. T. Verdeyen, Appl. Phys. Letters **6**, 185 (1965).

[9] R. W. McWhirter, *Plasma Diagnostic Techniques* (Academic Press Inc., New York, 1965), Chap. 5.

[10] H. Griem, *Plasma Spectroscopy* (McGraw-Hill Book Company, Inc., New York, 1964), Chap. 6.

[11] F. Robben, W. B. Kunkel, and L. Talbot, Phys. Rev. **132**, 2363 (1963).

[12] H. Chuang, Appl. Opt. **4**, 1589 (1965).

TABLE I. Recombination coefficients for 0.6 Torr of argon at $R=0$ with corresponding plasma parameters.

α cm^3 sec^{-1}	N_e cm^{-3}	T_e°K (Spectral)	α(Bates)	T_e°K (theor)
1.2×10^{-10}	2.6×10^{14}	2600	7.0×10^{-10}	3900
0.66×10^{-10}	4.6×10^{14}	3150	4.0×10^{-10}	5050
0.28×10^{-10}	8.8×10^{14}	3800	2.7×10^{-10}	7080

predetermined time following initiation of the discharge. This guaranteed that all measurements were made during the afterglow rather than the active discharge.

RESULTS AND DISCUSSION

The temporal and spatial variations of the electron and neutral-atom density for a typical discharge are shown in Fig. 2. Note that there is a strong depletion of the neutral-atom density along the tube axis and a slow relaxation back towards the equilibrium value. Because of the nonuniform distribution of the neutral-gas density, the electron-loss-rate equation assumes the following form:

$$\partial N_e/\partial t=\nabla\cdot(D_a\nabla N_e)-\alpha N_e^2, \qquad (1)$$

where D_a is the ambipolar diffusion coefficient, N_e is the electron density, α is the recombination coefficient. It should be recognized that D_a will be a function of both position and time due to the spatial nonuniformity of N_a. Hence the usual mode analysis is of limited value. Irrespective of this fact, both the temporal and spatial variations of the electron density can be directly evaluated from the data such as shown in Fig. 2. In this manner, the relative importance of the diffusion and the recombination losses can be estimated at all radial positions in the discharge tube.

Table I shows some representative values of the measured recombination coefficient and the corresponding electron density. These particular values are relative to the discharge tube axis. In obtaining these values due consideration was given to the diffusion term as given in Eq. (1). In order to accomplish this, one must know the electron temperature and for this we used, as a first approximation, the spectrally determined electron temperature. By an iterative procedure one can estimate the electron loss due to diffusion as a function of radial position. The recombination coefficient thus obtained is tabulated in the first column of Table I. The local neutral-atom density was measured by the laser interferometer as previously discussed and we assumed that the gas and ion temperatures were 600°K. This estimate for the gas temperature was obtained by assuming a constant gas pressure throughout the discharge vessel and using $T_{\text{gas}}=P/kN_a$.

Comparison of α in Table I with the collisional radiative recombination coefficient as calculated by Bates *et al.* indicates approximate agreement between theory and experiment. These theoretical values for the particular N_e and T_e are illustrated in column 4 of

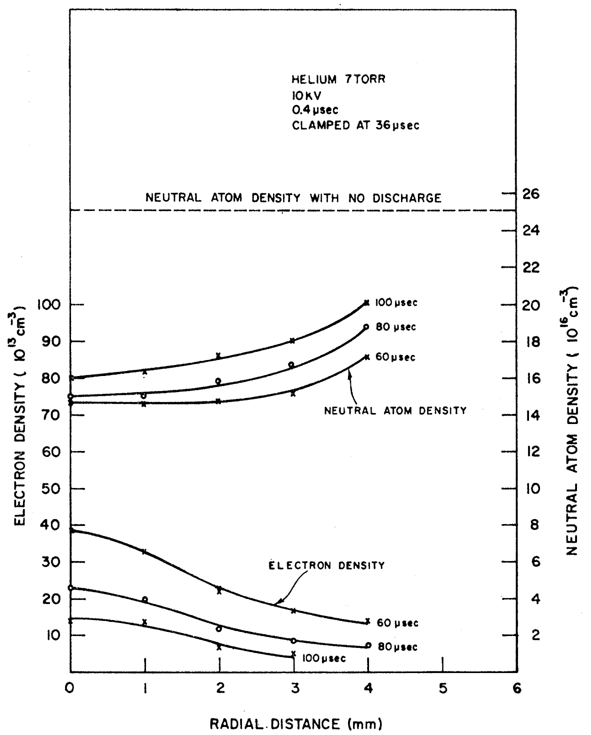

FIG. 2. Electron and neutral atom density as a function of radius in helium at 7 Torr.

Table I. Although not shown, such comparisons were made for all radial positions and various experimental conditions (gas pressure, discharge energy, time in afterglow, etc.).

Comparison of the experimentally obtained α to the value calculated by Bates *et al.* for collisional radiative recombination can also be made in a slightly different manner which proved to be more meaningful. In this comparison we determined at what temperature the experimental α agreed with the calculated value, and we designate the temperature as T_e°K (theor). This temperature is illustrated in column 5 of Table I. Comparison of T_e (theor) with T_e (spectral) is seen to be quite good, especially when one recalls that T_e (theor) corresponds to the electron temperature along the discharge tube axis and T_e (spectral) corresponds to some type of average value of the electron temperature along the tube diameter. From the radial dependence of α shown in Fig. 3, it was concluded that a nonuniform electron temperature exists across the plasma in the afterglow. The error bars in Fig. 3 are indicative of the experimental accuracy involved. Such errors have not been included near the discharge axis in order to maintain figure clarity; however, it might be mentioned that due to the increased importance of diffusion at the discharge axis, the corresponding error in determining $\alpha(R=0)$ will be larger than that at say $R=3$. From the measured $\alpha(R,t)$, T_e (theor) is shown in Fig. 4. It is important to realize that the spectral observation was

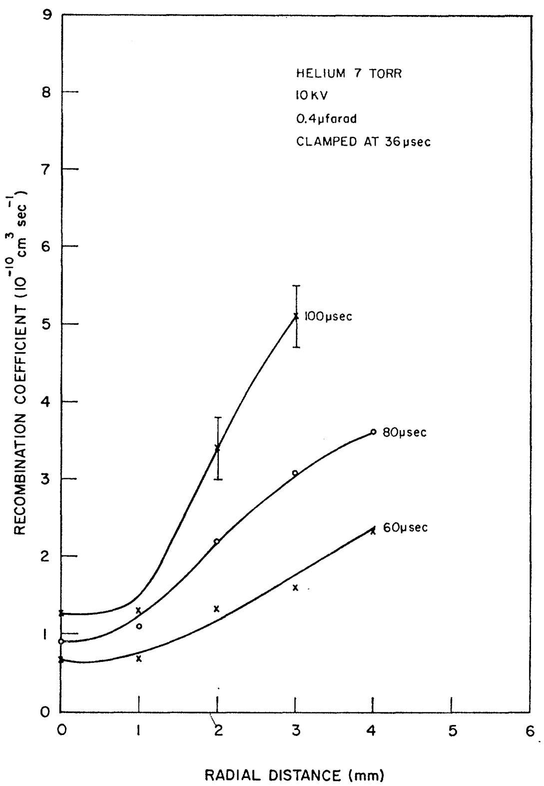

FIG. 3. Recombination coefficient as a function of radius at 7-Torr helium.

taken perpendicular to the discharge axis and thus is indicative of an "average" electron temperature. The spatial average of the inferred electron temperature was taken at various times in the afterglow. The results of this are shown in Figs. 5 and 6. There is quite acceptable agreement between the spectral temperature and the spatial average of the inferred temperature. With this understanding, it can be said that good agreement between the experiment and collisional-radiative recombination theory was found in helium, argon, and helium-argon mixtures. Over the times shown (and hence N_e and T_e), there appears to be no inconsistency between a $T_e^{-9/2}$ dependence of α and the experimental values.

It was quite unexpected that an electron temperature gradient should exist in an afterglow plasma at the relatively high electron densities involved. If, for example, one were to approximate the energy-balance equation by a normal-mode solution for the electron temperature as follows:

$$\frac{d}{dt}(\tfrac{3}{2}N_e k T_e) = \nabla\cdot(\kappa\nabla T_e) \approx -\frac{\kappa}{l^2}T_e,$$

where κ is the coefficient of thermal conductivity and l is the characteristic discharge length, and if the time dependence of N_e is neglected, then one would expect T_e to become uniform in approximately 10^{-7} sec for typical experimental conditions encountered here. Notice, however, that this order of magnitude is obtained in the absence of heating sources. In the presence of a nonuniform heating source of sufficient strength compared to cooling mechanisms it is quite possible for a nonuniform temperature distribution to exist. A simple analogy would be that of a hot soldering iron in contact with a copper sheet. In the afterglow described there are certainly heating sources which are in fact spatially nonuniform. Some of the possible heating and cooling mechanisms considered were:

I. Cooling

A. Thermal diffusion

$$\nabla\cdot\kappa\nabla T_e$$

B. Diffusion cooling

$$\nabla\cdot\gamma\nabla N_e,$$

where γ is the effective ambipolar diffusion cooling coefficient.

C. Electron-neutral and electron-ion elastic losses $-2m/M(\nu_{\rm en}+\nu_{\rm ei})\frac{3}{2}N_e k(T_e-T_g)$ (assume that $T_i=T_g$) where $\nu_{\rm en}$ and ν_{ei} are the electron-neutral and electron-ion elastic collision frequencies, respectively.

D. Inelastic collisions

$$X(p)+e\rightarrow X(q)+(e-\Delta E)\quad q>p,$$
$$\downarrow$$
$$X+h\nu$$

where ΔE is the energy increment obtained from energy balance.

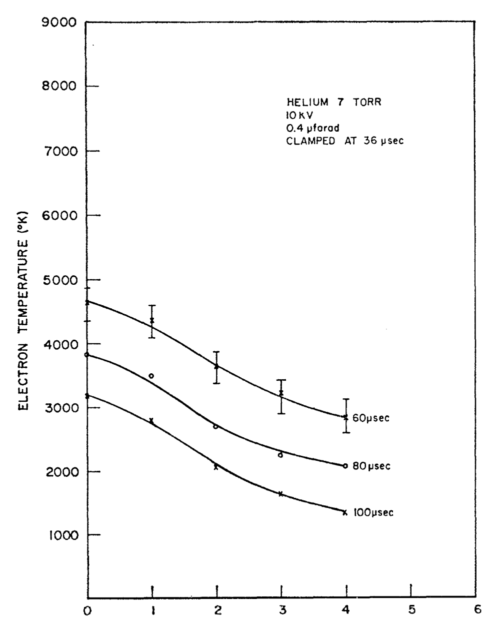

FIG. 4. Electron temperature as a function of radius for 7-Torr helium.

II. Heating

A. Recombination heating (see Appendix)

$$X^+ + e + e \rightarrow X(p) + (e + \Delta E)$$

B. In helium, singlet-triplet superelastic conversion

$$2^1S + e \rightarrow 2^3S + (e + \Delta E)$$

C. Superelastic metastable–ground-state transitions

$$X_m + e \rightarrow X + (e + \Delta E)$$

D. Metastable-metastable collisions

$$X_m + X_m \rightarrow X^+ + X + (e + \Delta E)$$

Order-of-magnitude calculations indicate that the dominant processes in this work are IA, IIA, IIB, and IID. If in fact IID is important, then our determination of the recombination coefficient will be an effective lower bound in this regard, since this process produces free electrons. It has been shown by Ingraham and Brown[13] that heating due to singlet-triplet conversion and metastable-metastable collisions can be important heating mechanisms. Recombination heating under the conditions of the present work is typically about 2.00 eV per recombination event (see Appendix). Singlet-triplet conversion supplies 0.8 eV per super-elastic collision. The mentioned order-of-magnitude calculations indicate that the total heating rate is the same order of magnitude as the total cooling rate. Thus a relatively slow decay of the spatially nonuniform electron temperature in the afterglow is understandable.

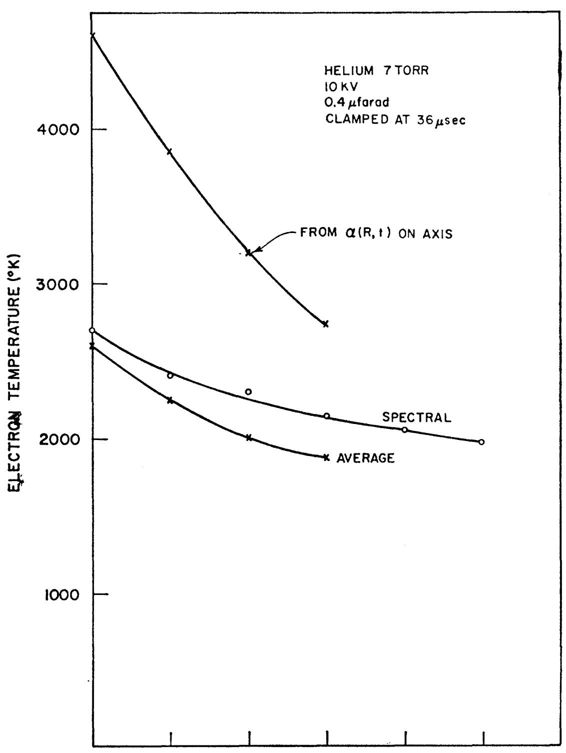

FIG. 5. Eletron temperature as a function of time for 7-Torr helium.

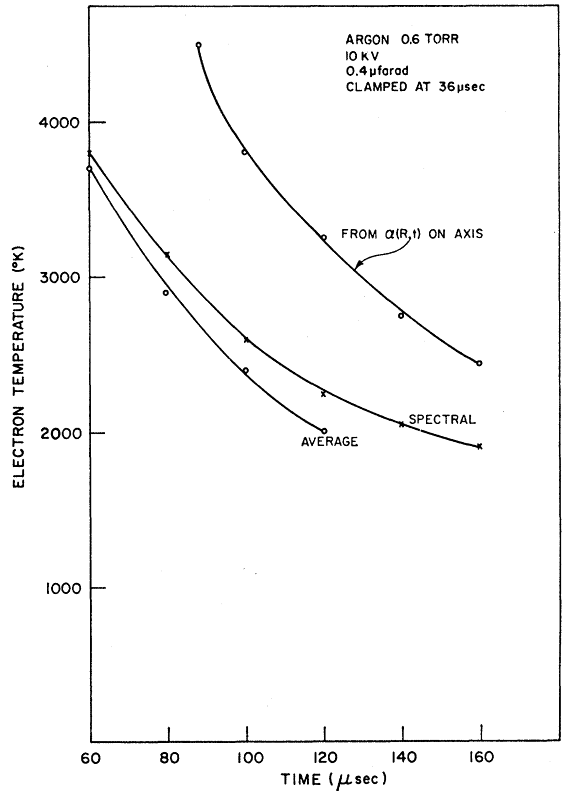

FIG. 6. Electron temperature as a function of time for 0.6-Torr argon.

CONCLUSIONS

It was found that in the ranges $2\times10^{13} < N_e \leq 10^{15}$ cm^{-3} and $1000°K \leq T_e \leq 8000°K$ the recombination process in helium, argon, and helium-argon mixtures is consistent with the present theory of collisional-radiative recombination. The recombination appears to be essentially independent of the type of single ionized atom, in agreement with theory. It was found that a nonuniform electron-temperature profile existed across the discharge cross section in the afterglow. It is believed, from qualitative and semiquantitative arguments, that spatially nonuniform electron-gas heating in the afterglow is responsible for this behavior.

The existence of nonuniform neutral-atom densities and a nonuniform electron temperature across the discharge complicate diffusion. The electron-loss equation is not solvable in terms of elementary functions and must be solved in conjunction with the energy-balance

[13] J. C. Ingraham and S. C. Brown, Phys. Rev. 138, A1015 (1965).

equation. Because of the complexity and coupling between these two equations it is not meaningful to discuss mode solutions or time constants in the usual sense.

To date, there appear to be three likely candidates to explain observation of recombination made on laboratory plasmas. These are (a) collisional-radiative recombination, (b) collisional-dissociative recombination, and (c) two-body dissociative recombination. At the present time all three mechanisms appear to be important. It is likely that the difficulties encountered in the past concerning recombination studies stem from the tendency of the investigators to attempt to explain their observations under essentially all electron density and temperature ranges by a single process. The type of recombination process dominating the electron loss depends on the plasma conditions. It is reasonable to expect that, under the appropriate conditions, there may be several types of recombination occurring.

ACKNOWLEDGMENT

The authors wish to thank Dr. L. Goldstein for several helpful discussions.

APPENDIX

Recombination Heating

To calculate the recombination heating, the following reaction is used:

$$\begin{array}{ccccc} X^{+}+e & +e & \rightarrow X(p) & +e \\ I \quad\; E & E' & I-E_p & E_p+E+E' . \end{array}$$

The appropriate energetics are indicated below the reaction. The excess energy supplied to the electron gas is E_p+E. The average excess energy supplied to the electron gas per capture to the pth state from the continuum is

$$\bar{\epsilon}_p=\int_0^\infty {}^c\sigma_p(E)f(E)(E+E_p)E\,dE \Big/ \int_0^\infty {}^c\sigma_p(E)f(E)E\,dE ,$$

where ${}^c\sigma_p$ is the superelastic cross section for the reaction $c\rightarrow p$ (c refers to the continuum) and $f(E)$ is the free-electron distribution function. The superelastic cross section is not directly known; however, if the inverse inelastic cross section is known, then, from detailed balancing,

$${}^c\sigma_p(E)={}_p\sigma^c(E+E_p)((E+E_p)/E) .$$

If the classical Thomson inelastic cross section is used

$${}_p\sigma^c(E)=\pi e^4E^{-1}(E_p^{-1}-E^{-1})\mu(E-E_p) ,$$

then it is found that

$${}^c\sigma_p(E)=\pi e^4E_p^{-1}(E+E_p)^{-1}\mu(E) ,$$

where $\mu(E-E_p)$ and $\mu(E)$ are unit step functions to account for threshold. Taking the electron gas to be described by a Maxwellian distribution, it is found that

$$\bar{\epsilon}_p=E_p+kT_e ,$$

where T_e is the free-electron temperature.

Now, to find the average recombination energy supplied to the electron gas one must weight $\bar{\epsilon}_p$ and sum over all possible capture states.

$$\bar{\epsilon}=\textstyle\sum_p {}^cR_p\bar{\epsilon}_p/\sum_p {}^cR_p ,$$

where ${}^cR_p$ is the rate of superelastic transitions $c\rightarrow p$. Using a hydrogenic model, one finds from Hinnov and Hirschberg[2]

$${}^cR_p=7.75\times10^{-27}(kT_e)^{-2}N_e^3E_p^{-2} ,$$

where kT_e and E_p are in units of eV. States within kT_e of the continuum need not be considered in the sum over states since these closely lying states will be in local thermodynamic equilibrium with the free-electron gas. As a result there will be no net exchange of energy bebetween such states and the free electrons. Replacing the summations by integrals, it is found that

$$\bar{\epsilon}\approx kT_e(\ln(I/kT_e)+1) .$$

For example, for a plasma with an electron temperature of 4000°K,

$$\bar{\epsilon}\text{ (helium)}\approx1.98\text{ eV} ,$$
$$\bar{\epsilon}\text{ (argon)}\approx1.80\text{ eV} .$$

Besides the mathematical approximations involved, the above is only an estimate since a hydrogenic model was used. It is important to notice that to obtain a more accurate picture one should take account of radiative transitions from the continuum to bound states as well as re-ionization from bound states. Superelastic and inelastic collisions involving bound levels should also be treated. It might be mentioned that Byron *et al.*[14] have estimated the recombination heating and at $T_e=4000$°K. Their results indicate $\bar{\epsilon}\gtrsim1.12$ eV.

[14] S. Byron, R. C. Stabler, and P. Bortz, Phys. Rev. Letters 8, 376 (1962).